

ORIGINAL INVESTIGATION

Open Access



# Dual inhibition of sodium–glucose linked cotransporters 1 and 2 exacerbates cardiac dysfunction following experimental myocardial infarction

Kim A. Connelly, Yanling Zhang, Jean-François Desjardins, Kerri Thai and Richard E. Gilbert\* 

## Abstract

**Background:** Inhibiting both type 1 and 2 sodium–glucose linked cotransporter (SGLT1/2) offers the potential to not only increase glucosuria beyond that seen with selective SGLT2 inhibition alone but to reduce glucose absorption from the gut and to thereby also stimulate glucagon-like peptide 1 secretion. However, beyond the kidney and gut, SGLT1 is expressed in a range of other organs particularly the heart where it potentially assists GLUT-mediated glucose transport. Since cardiac myocytes become more reliant on glucose as a fuel source in the setting of stress, the present study sought to compare the effects of dual SGLT1/2 inhibition with selective SGLT2 inhibition in the normal and diseased heart.

**Methods:** Fischer F344 rats underwent ligation of the left anterior descending coronary artery or sham ligation before being randomized to receive the dual SGLT1/2 inhibitor, T-1095, the selective SGLT2 inhibitor, dapagliflozin or vehicle. In addition to measuring laboratory parameters, animals also underwent echocardiography and cardiac catheterization to assess systolic and diastolic function in detail.

**Results:** When compared with rats that had received either vehicle or dapagliflozin, T-1095 exacerbated cardiac dysfunction in the post myocardial infarction setting. In addition to higher lung weights, T-1095 treated rats had evidence of worsened systolic function with lower ejection fractions and reduction in the rate of left ventricle pressure rise in early systole ( $dP/dt_{max}$ ). Diastolic function was also worse in animals that had received T-1095 with prolongation of the time constant for isovolumic-pressure decline ( $\tau$ ) and an increase in the end-diastolic pressure volume relationship, indices of the active, energy-dependent and passive phases of cardiac relaxation.

**Conclusions:** The exacerbation of post myocardial infarction cardiac dysfunction with T-1095 in the experimental setting suggests the need for caution with the use of dual SGLT1/2 inhibitors in humans.

**Keywords:** Sodium–glucose linked cotransporter, Myocardial infarction, Systole, Diastole

## Background

Sodium–glucose linked cotransporter-2 inhibitors (SGLT2i) increase urinary glucose excretion thereby off-loading energy, lowering plasma glucose and body weight as well as inducing a modest diuresis that reduces extracellular fluid volume and lowers blood

pressure. In addition, two recent cardiovascular outcome studies with these agents demonstrated reductions in heart failure hospitalisation suggesting that this class of drug exerts cardioprotective effects beyond glucose and blood pressure lowering [1, 2].

In addition to SGLT2, another glucose transporter, SGLT1, cotransports sodium and glucose in the distal segment of the proximal tubule with higher affinity and lower capacity than its more proximal counterpart. Unlike SGLT2, whose expression is confined to

\*Correspondence: richard.gilbert@utoronto.ca  
Keenan Research Centre, Li Ka Shing Knowledge Institute, St. Michael's Hospital, 61 Queen Street East, Toronto, ON M5C 2T2, Canada



the kidney, SGLT1 is also abundantly present in the gut where it accounts for much of glucose (and galactose) absorption by enterocytes. Accordingly, combined SGLT1/2 inhibition offers the potential to not only increase glucosuria beyond that seen with SGLT2 inhibition alone but to reduce glucose absorption allowing the monosaccharide to stimulate release of glucagon-like peptide-1 (GLP-1) in the ileum. As such, dual SGLT1/2 inhibition presents an appealing strategy for glucose lowering in diabetes with drugs that do so currently in development [3].

Beyond its expression in the kidney and small intestine, however, SGLT1 is also present in various other organs in humans including the lung, liver, pancreatic alpha cells, skeletal muscle and particularly in the heart where its abundance exceeds that of the kidney [4–6]. Similar high expression levels have recently also been reported in the hearts of rats and mice [7]. With its constant and high energy requirements and little storage capacity, the heart requires a constant supply of energy-generating substrates. This is especially important during ischaemia when the ability to generate more ATP per O<sub>2</sub> molecule consumed and to also generate ATP anaerobically by glycolysis render glucose preferable to fatty acids as a substrate for energy production [8]. Although the facilitated glucose transporters GLUT1 and GLUT4 were previously thought to account entirely for glucose transport in the heart, more recent studies attest to the additional contribution of SGLT1 [9–12].

Given their potential to enter the clinical arena, we sought to examine the effects of dual SGLT1/2 inhibition in experimental heart disease using the rat coronary artery ligation model that develops ischemia, infarction and heart failure. Accordingly, the primary objective of the study was to assess changes in cardiac function and secondarily changes in structure. To avoid the requirement for longterm parenteral administration with the poorly absorbed and rapidly metabolized phlorizin, we administered the readily absorbed SGLT1/2 dual inhibitor prodrug, T-1095, that is quickly converted to the active moiety, T-1095A following its entry into the systemic circulation [13, 14].

## Methods

### Animals

Ninety-nine 7-week old male rats Fischer F344 rats (Charles River Laboratories, Wilmington, MA, USA) were randomized to myocardial infarction or sham groups in a ratio of 3:1 using the left anterior descending (LAD) coronary artery of myocardial infarction that provides a robust model of adverse cardiac remodeling akin to its human counterpart [15]. Animals were then

further randomized in a ratio of 1:1:1 to receive either vehicle, the dual SGLT1/2 inhibitor, T-1095 (150 mg/kg/day, Sun-Shine Chemical Technology Co., Ltd, Shanghai, China) dosed as previously described [16], or the selective SGLT2 inhibitor, dapagliflozin 0.5 mg/kg b.i.d (gift of Astra Zeneca, Gothenburg, Sweden) [17] by gavage. Doses of T-1095 (150 mg/kg/day or 0.1 wt/wt admixed in chow) and dapagliflozin (1 mg/kg/day) were based on previously published literature according to their ability to achieve an approximate 50% reduction in plasma glucose when administered to diabetic rats [18, 19].

Myocardial infarction was induced 1 week later by ligation of the LAD coronary artery with sham animals undergoing thoracotomy and incision of the pericardial sac, but not LAD ligation [20]. Two days later, rats underwent echocardiography, and were randomized on confirmation of MI and demonstration of similar MI size based upon fractional shortening and wall motion score index [21] and followed for a further 7 weeks before being terminated. All procedures were performed in the research vivarium under anesthesia using 2.5% isoflurane supplemented with 100% O<sub>2</sub> as previously undertaken and shown to effectively reduce consciousness without impairing cardiac function [22]. Urine was obtained for measurement of glucose concentration just prior to termination by cervical dislocation under isoflurane anesthesia. Because of the comparatively short duration of the study in comparison with the half-life of erythrocytes, fructosamine rather than hemoglobin A<sub>1c</sub> was used provide an integrated index of glycemia. Serum fructosamine concentrations was, accordingly, determined by colorimetric assay using a commercial diagnostic assay (Roche Diagnostics, Canada) analyzed on the Olympus AU400 automated chemistry analyzer (Beckman Coulter, Canada).

Animals underwent echocardiography and cardiac catheterization as described below. Following these procedures, rats were terminated and their hearts and lungs removed for weighing and other assessments, as also described below. Tibial length was measured to provide a morphometric index for cardiac hypertrophy and lung weight [23].

Sample size estimates were based on similar studies previously reported by our group using this animal model [24]. Of the cohort of 99 rats, five did not show evidence of wall motion abnormalities indicative of infarction when echocardiography was performed 2 days after LAD ligation. A further 17 (8 from the vehicle group and 9 from the dapagliflozin group) died during surgery or during the immediate postoperative recovery period following myocardial infarction. Two post-MI animals were withdrawn from the study when it became evident that there were insufficient quantities of T-1095

for them to complete. As such, the final number of animals that completed the study as per protocol were 22, 13 and 15 among the MI+vehicle, MI+dapagliflozin and MI+T-1095 groups, respectively and 12, 7 and 6 among the sham+vehicle, sham+dapagliflozin and sham+T-1095 groups, respectively.

All animals were housed 2/cage at the St. Michael's Hospital Animal Research Vivarium in a temperature-controlled (22 °C) room with a 12-h light/dark cycle and ad libitum access to commercial standard rat chow. Enrichment, proper animal handling and anesthesia procedure were used to minimize the pain and distress of the animals during the study. All animal studies were approved by the St. Michael's Hospital Animal Care Committee in accordance with the Guide for the Care and Use of Laboratory Animals (NIH Publication No. 85-23, revised 1996).

### Echocardiography

Transthoracic echocardiography was performed, as previously described [25], under light anaesthesia (1% isoflurane supplemented with 100% O<sub>2</sub>), at 2 days and 8 weeks post MI, prior to sacrifice. Images were acquired using a high-frequency ultrasound system (Vevo 2100, MS-250 transducer, Visualsonics, Toronto, ON). Two dimensional long-axis images of the LV in parasternal long- and short-axis views with M-mode measurements at mid-papillary muscle level and linear dimensions were analyzed offline (Vevo 2100 software v. 1.8) using the standard leading edge-to-leading edge technique by a single investigator, masked to treatment.

MI size was estimated 2 days after LAD ligation by measuring the percentage of endocardial circumferential extent of LV akinesis at end-diastole using 2D short-axis images of the LV at mid-papillary muscle level. Corrected LV mass was calculated using the Devereux and Reichek "cube" formula that includes a 20% correction for over-estimation of LV mass based on data derived from previously reported validation studies [26, 27]. Fractional shortening (FS%) was calculated according to the formula:  $FS\% = (LVIDd - LVIDs) / LVIDd \times 100$ , where LVIDd and LVIDs are end-diastolic diameter and end-systolic diameter respectively, as previously described [28]. Three consecutive cardiac cycles were averaged for all analyses.

### Cardiac catheterization

Cardiac catheterization was performed as previously published [25]. Briefly, rats were anaesthetized with 2.5% isoflurane, intubated using a 14 gauge catheter and ventilated using a pressure controlled ventilator (TOPO ventilator, Kent Scientific, Torrington, CT). Adequacy of anaesthesia was assessed by lack of response to surgical

manipulation and loss of muscular tone. Rats were placed in the supine position on a water circulating heating pad and a 1.4 F pressure-volume (PV) catheter (SPR-838; Millar Instruments, Inc., Houston, TX) was inserted into the right carotid and advanced into the left ventricle and PV loops were generated. All pressure-volume (PV) loops were obtained with the ventilator turned off for 5–10 s and the animal apnoeic.

Data were acquired and recorded with a MPVS ultra<sup>®</sup> data acquisition system (Millar Instruments) and Lab-Chart Pro software (CHART 8.1 ADInstruments Inc., Colorado Springs, CO) under steady-state and following inferior vena cava occlusion (preload reduction). Conductance signals acquired with the Millar catheter were calibrated with estimated LV volumes derived echocardiographically using a two-point calibration method, matching LV maximal and minimal conductance signals and end-diastolic and end-systolic volumes (EDV and ESV) measured in long-axis view for each individual rat, respectively. Using the pressure conductance data, a range of functional parameters were then calculated.

### Histopathology

To determine the extent of extracellular matrix deposition, sections were stained with antibodies to types I and III collagen (Southern Biotech, Birmingham, AL). The abundance of matrix within the non-infarct zone was then quantified as previously described [29]. To isolate the non-infarct zone from the infarct and the peri-infarct zone, the infarct and a 2 mm zone on either side of it were excluded from analysis. The proportional area staining brown within the remaining myocardium composed the non-infarct zone was then assessed using computer-assisted image analysis (Aperio ImageScope, Leica Biosystems Inc., Concord, Ontario, Canada), as previously described [30]. The whole non-infarct zone was used for quantification of ECM in order to prevent possible bias from using selected fields. For sham animals, the ECM content of the entire LV was quantitated by the same method, as described above.

The extent of cardiac myocyte hypertrophy was determined on haematoxylin and eosin stained sections, as previously reported [31]. In brief, stained sections were scanned with the Aperio Ultra-Resolution Digital Scanning System (Aperio Technologies Inc., Vista, CA), and the images were analyzed with The NDP.view2 viewer software (Hamamatsu Photonics, Hamamatsu City, Shizuoka Pref., Japan). Cardiac myocytes with elliptical nuclei in transverse section were selected. Diameter measurements were taken membrane to membrane across the narrowest point that crosses the nucleus. The average diameter of 30–50 myocytes per animal was measured based on the method previously reported [32].

**Western blot**

The abundance of SGLT 1 and 2 were assessed by immunoblot, as previously described [33] using specific isoform antibodies (Santa Cruz Biotechnology, Dallas, TX). In brief, small pieces of heart tissue were rapidly collected from the non-infarct zone, snap frozen in liquid nitrogen and stored at -80 °C until use. Lysates were prepared by homogenizing frozen heart tissue in ice-cold lysis buffer (50 mM Tris, pH 7.4, 150 mM NaCl, 1 mM EDTA, 1 mM EGTA, 0.5% Triton X-100 containing 1 mM Na<sub>3</sub>VO<sub>4</sub>, 50 mM NaF, 25 mM β-glycerophosphate, 10 mM Na pyrophosphate, 10 μg/ml aprotinin, 10 μg/ml leupeptin, 1 mM PMSE, 1 mM DTT). After 30 min incubation on ice, lysates were centrifuged to remove cell debris. Protein concentration was determined using Bradford reagent (Bio-rad, Hercules, CA) and standardized with known amounts of BSA. Western blot analysis was performed by resolving 50 μg of total protein on a 10% SDS-polyacrylamide gel by denaturing discontinuous gel electrophoresis according to the Laemmli method, and transferring to PVDF membranes (Roche, Mannheim, Germany). After incubating in blocking solution (5% nonfat dry milk, Tris buffered saline (pH 7.5), 0.1% Tween 20), membranes were immunoblotted with primary antibodies at 1:1000 dilution overnight at 4 °C. Membranes were then washed three times (5 min each) with TBST and blots were incubated with HRP-conjugated secondary antibodies (Dako) for 1 h at room temperature. The membranes were washed three times, and proteins were detected by the ECL system (Roche). Rat kidney served as positive control for SGLT2. Signals were digitized then analyzed with ImageJ software (NIH, Bethesda, MD). Results were calculated as the mean of at least three experiments relative to β-actin immunolabeling. Kidney homogenates served as positive controls for both SGLT1 and -2.

**Gene expression**

The abundance of atrial natriuretic peptide (ANP) was assessed by measuring its mRNA by quantitative real-time PCR in left ventricular tissue stored at -80 °C as previously described [34]. In brief, SYBR green-based measurement of gene expression were performed on QuantStudio 7 Flex Real-Time PCR System (Applied Biosystems, Foster City, CA) according to the manufacturer’s instructions using the predesigned sequence-specific primers for ANP from Integrated DNA Technologies (Coralville, IA). Data were analyzed using Applied Biosystems Comparative CT method.

**Statistics**

Data are expressed as mean ± SEM unless otherwise specified. Between group differences were analyzed by one way ANOVA with Fisher’s Protected Least Significant Difference test post hoc. All statistics were performed using GraphPad Prism 6 for Mac OS X (GraphPad Software Inc., San Diego, CA). A p value of <0.05 was regarded as statistically significant.

**Results**

**Morphometric characteristics**

No differences in baseline in body weight among the six groups were evident prior to randomization. When compared with rats that had been treated with dapagliflozin, those randomized to receive T-1095 had lower body weights in the post-MI setting (Table 1). Left ventricular weight, indexed to tibial length, increased following myocardial infarction with lower values noted in rats that had received dapagliflozin but lower still in those randomized to T-1095. Lung weight indexed to tibial length was increased in all animals that had undergone coronary artery ligation but to a greater extent in rats that had received T-1095 compared with dapagliflozin-treated animals.

**Table 1 Animal characteristics and laboratory parameters**

	sham + vehicle	sham + dapa	sham + T-1095	MI + vehicle	MI + dapa	MI + T-1095
N	12	7	6	22	13	15
BW (g)	305.3 ± 3.8	281.3 ± 3.3*	248.3 ± 8.1*	299.9 ± 3.1	282.8 ± 5.0*†	263.5 ± 4.2*†
LV W/TL (g/mm)	14.8 ± 0.1	13.4 ± 0.1*	12.2 ± 0.3*	15.9 ± 0.2*	15.0 ± 0.2†	14.1 ± 0.4†
Lung W/TL (g/mm)	27.4 ± 0.5	26.8 ± 0.3	24.7 ± 0.4	43.7 ± 3.9*	40.3 ± 4.4*	54.2 ± 5.0*†
UG (mmol/l)	0.34 ± 0.07	316.0 ± 34.3*	256.2 ± 66.6*	0.21 ± 0.03	235.0 ± 10.3*†	205.2 ± 21.6*†
Fructosamine (μM)	141.8 ± 3.3	126.2 ± 2.4*	129.2 ± 2.8*	121.5 ± 3.3*	122.5 ± 2.0*	130.8 ± 4.4*†
ANP: RPL13a mRNA (AU)	1.09 ± 0.23	1.39 ± 0.44	1.52 ± 0.23	13.02 ± 2.33*	7.47 ± 1.15*†	9.61 ± 1.07*

BW body weight, SBP systolic blood pressure, LVW left ventricle weight, TL tibia length, Lung W lung weight, BG blood glucose, UG urinary glucose, ANP atrial natriuretic peptide, RPL13a Ribosomal Protein L13a, AU arbitrary units, dapa dapagliflozin

\* p < 0.05 vs. sham + vehicle group; † p < 0.05 vs. MI + vehicle group



**Laboratory and molecular parameters**

Fructosamine concentrations were lower in both dapagliflozin and T-1095 when compared with vehicle-treated control animals. In rats that had undergone LAD ligation, however, fructosamine concentrations were lower than

in vehicle-treated control animals though less so among rats that had received T-1095 (Table 1). No glucosuria was detected in untreated animals but was readily apparent in animals that received either T-1095 or dapagliflozin (Table 1). SGLT1 was easily detected by immunoblot of cardiac tissue but was unaffected by either myocardial infarction or treatment group assignment (Fig. 1). SGLT2 on the other hand, while abundantly expressed in the kidney could not be detected in cardiac tissue (data not shown).

The expression of ANP mRNA was assessed as a marker of extracellular fluid volume and cardiac wall stress. Its abundance was increased in the hearts of all animals that had undergone experimental myocardial infarction but less so in those that had received dapagliflozin when compared with either vehicle or T-1095 treated rats (Table 1).

**Echocardiography**

Ejection fraction and fractional shortening were reduced in all animals that undergone experimental myocardial infarction when compared with sham surgery animals (Fig. 2, Table 2). Ejection fraction was, however, reduced to an even greater extent in those rats that had received T-1095 than those treated with either vehicle or dapagliflozin. Similar changes were also noted in left ventricular mass that while increased in all groups that had undergone LAD ligation, this was less so in those that had received T-1095 when compared with either vehicle- or dapagliflozin-treated animals.

**Conductance catheterization**

Global left ventricular contractility, as measured by the rate of left ventricle pressure rise in early systole ( $dp/dt_{max}$ ), was reduced in the post-MI setting but to a greater extent in those that had received T-1095 when

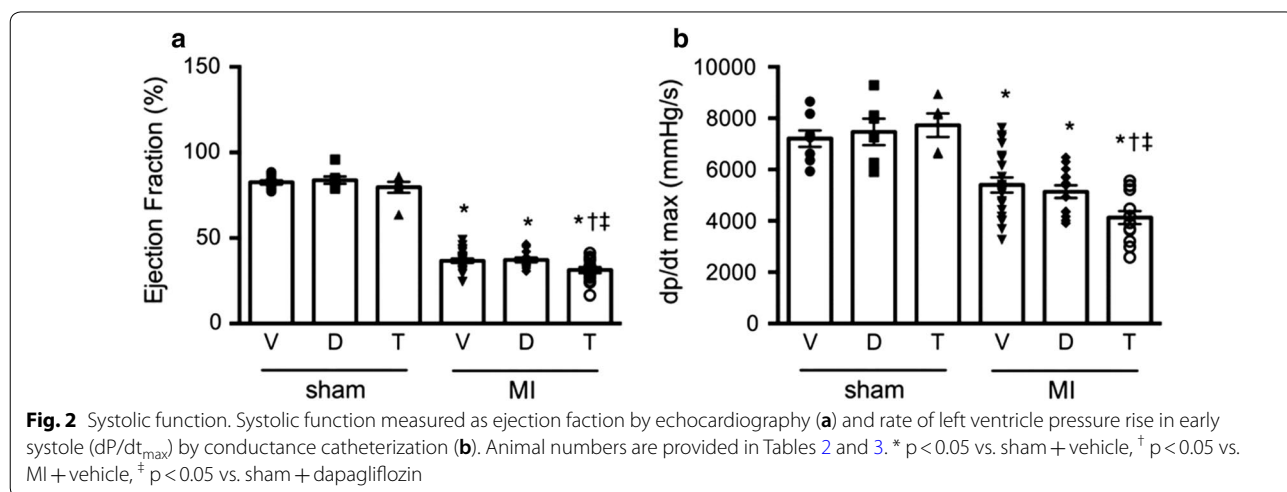
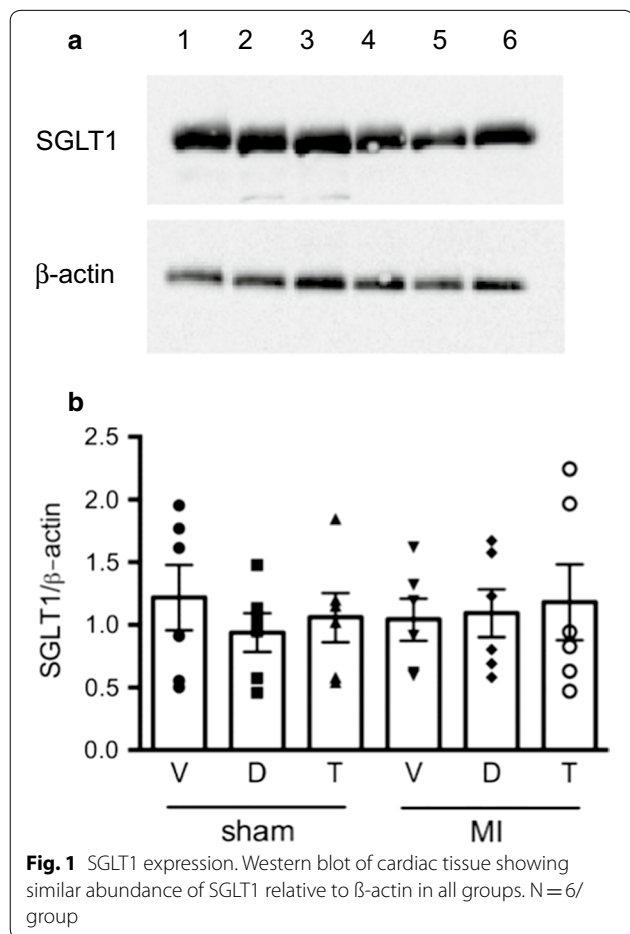


**Table 2 Echocardiographic parameters**

	sham + vehicle	sham + dapa	sham + T-1095	MI + vehicle	MI + dapa	MI + T-1095
N	12	7	6	20	12	14
MI size (%)	–	–	–	44 ± 2	38 ± 2	40 ± 2
FS (%)	53 ± 1	55 ± 3	50 ± 3	19 ± 1*	19 ± 1*	16 ± 1*
EF (%)	83 ± 1	84 ± 2	80 ± 3	37 ± 1*	37 ± 1*	31 ± 2*††
LV mass corr. (mg)	684 ± 26	608 ± 35*	578 ± 41	827 ± 36*	800 ± 41*	759 ± 39
LVIDd (mm)	6.73 ± 0.08	6.62 ± 0.18*	6.50 ± 0.07*	9.17 ± 0.15*	9.21 ± 0.18*	9.05 ± 0.11*
LVIDs (mm)	3.17 ± 0.09	3.01 ± 0.25	3.25 ± 0.18	7.47 ± 0.17*	7.48 ± 0.20*	7.64 ± 0.11*
Volume s (µl)	63 ± 4	52 ± 6	56 ± 10	359 ± 28*	371 ± 32*	402 ± 18*
Volume d (µl)	289 ± 15	272 ± 19	223 ± 13	574 ± 25*	555 ± 31*	556 ± 19*

EF ejection fraction, FS fractional shortening, LV mass corr left ventricle mass corrected, LVPW left ventricular posterior wall, LVIDd left ventricle internal diameter in diastole, LVIDs left ventricle internal dimension in systole

\* p < 0.05 vs. sham + vehicle group; † p < 0.05 vs. MI + vehicle group; †† p < 0.05 vs. MI + dapagliflozin group

compared with either vehicle or dapagliflozin-treated animals (Fig. 2, Table 3). The rapid, early decrease in LV pressure during the period of isovolumic relaxation ( $dp/dt_{min}$ ) that reflects diastolic function was also reduced in rats that had undergone LAD ligation (Fig. 3). The extent of the reduction differed according to treatment assignment with those animals randomized to receive T-1095 experiencing the greatest reduction. This same pattern was also evident in other indices of diastolic function including both Tau, that assesses the early energy-dependent phase of relaxation as well as the end-diastolic pressure volume relationship (EDPVR) that provides an index of passive LV compliance (Fig. 3, Table 3). Systolic blood pressure was similar in all groups with the exception of post-MI rats receiving T-1095 where it was slightly lower.

**Histopathology**

Myocyte dimensions differed according to treatment assignment. Animals that received T-1095 did not show

evidence of hypertrophy in the post-MI setting, contrasting those in rats randomized to vehicle or dapagliflozin (Fig. 4). The extent of fibrosis in the left ventricle in the area remote from the site of infarction also differed according to group assignment. Increased type III collagen was evident in the interstitium of those rats that had received either vehicle or T-1095 but not in those that had been treated with dapagliflozin (Figs. 5, 6). A different pattern was observed for type I collagen where increased deposition was only found in animals that had received T-1095 following experimental myocardial infarction (Figs. 5, 6).

**Discussion**

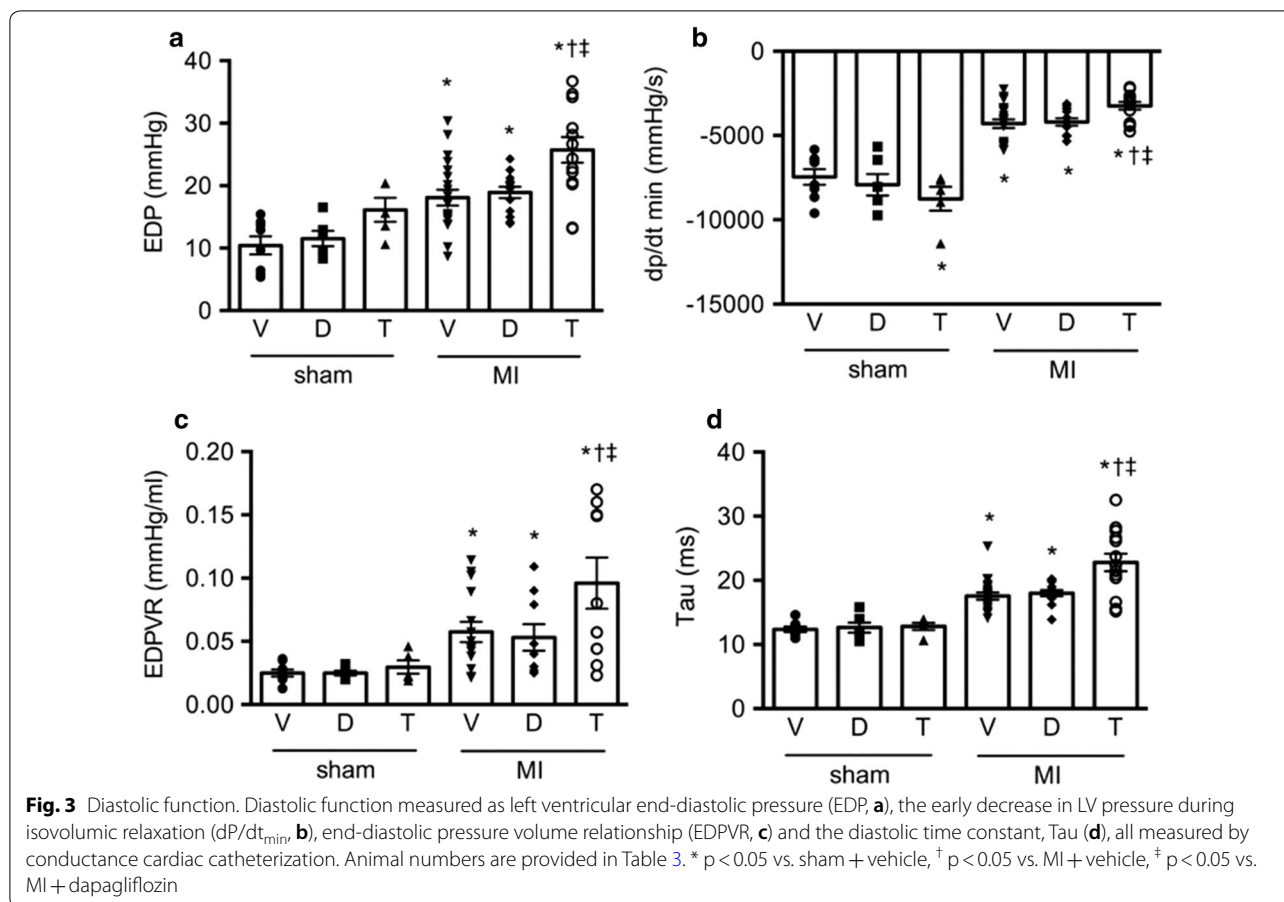
Unlike SGLT2 whose expression is almost exclusively confined to the kidney, SGLT1 is abundantly expressed in the heart. Blocking the SGLT2 transporter alone with dapagliflozin had no effect on cardiac function in either the control setting or after myocardial infarction. Dual blockade of SGLT 1 and 2 with T-1095, however, while not affecting function under physiological circumstances

**Table 3 Conductance catheterization**

	sham + vehicle	sham + dapa	sham + T-1095	MI + vehicle	MI + dapa	MI + T-1095
N	5	6	4	20	13	13
EDP (mmHg)	11 ± 2	12 ± 1	16 ± 2*	18 ± 1*	19 ± 1*†	26 ± 2*†
Pes (mmHg)	117 ± 11	127 ± 7	127 ± 15	107 ± 5	105 ± 5	95 ± 5*
HR (bpm)	296 ± 12	288 ± 12	299 ± 11	270 ± 7*	258 ± 6*	260 ± 9*
$dp/dt_{max}$ (mmHg/s)	7031 ± 426	7471 ± 514	7815 ± 504	5443 ± 305*	5141 ± 249*	4201 ± 264*††
$dp/dt_{min}$ (mmHg/s)	– 7190 ± 631	– 7922 ± 637	– 8927 ± 906*	– 4318 ± 260*	– 4192 ± 224*	– 3290 ± 246*††
EDPVR (mmHg/ml)	0.024 ± 0.004	0.025 ± 0.002	0.03 ± 0.01	0.06 ± 0.01	0.05 ± 0.01	0.10 ± 0.02*††
Tau (ms)	12.5 ± 0.6	12.6 ± 0.8	12.5 ± 0.7	17.5 ± 0.6*	18.0 ± 0.5*	23.2 ± 1.6*††

EDP end-diastolic pressure, Pes end-systolic pressure, HR heart rate, EDPVR end-diastolic pressure volume relationship, ESPVR end-systolic pressure volume relationship

\* p < 0.05 vs. sham + vehicle group; † p < 0.05 vs. MI + vehicle group; †† p < 0.05 vs. MI + dapagliflozin group



led to an exacerbation of impairment in both systole and diastole in the post myocardial infarction setting.

Ligation of the left anterior descending coronary artery leads to substantial infarction of the left ventricle, providing a well-established model of progressive heart failure in rodents [15]. As expected, all animals in the current study that had undergone ligation displayed evidence of systolic dysfunction. Notably, the key features of left ventricular function such as ejection fraction and  $dp/dt_{max}$  were both worse in the group that had received the SGLT1/2 inhibitor, T-1095 when compared with those treated with either vehicle or dapagliflozin. Similarly, diastolic function was also abnormal 4 weeks following LAD ligation but worse still among those rats that had received T-1095. Moreover, abnormalities in both the early, active, energy-dependent phase of diastole as indicated by prolongation of the diastolic time constant, Tau and the later, more passive phase of diastole as reflected by an increase in the end-diastolic pressure volume relationship (EDPVR) were also more severely affected in T-1095-treated animals.

Following ischaemic necrosis of the myocardium the heart undergoes adaptive (in addition to adverse)

remodelling in an attempt to compensate for the loss of contractile tissue. In this regard, an increase in left ventricular wall thickness as a consequence of myocyte hypertrophy reduces wall stress, as dictated by the Laplace law [35]. Notably, the requirement for anabolic growth in addition to maintaining ATP generation for cardiac contractility necessitates an increase in glycolytic flux [36]. In this setting, the role of SGLT1-mediated glucose entry into cardiac myocytes that can be inhibited by agents such as T-1095 becomes increasingly important [11, 37, 38]. Indeed, inhibition of cardiac hypertrophy in the setting of increased wall stress, as demonstrated in the present study would be predicted to be detrimental [39] as demonstrated by the cardiac dysfunction and reduced survival when hypertrophy is inhibited in experimental animals subjected to cardiac stress [40–44]. In contrast to the aforementioned primary inhibition of myocyte hypertrophy, ACE inhibitors and  $\beta$ -blockers reduce preload and afterload so that the need for hypertrophy is reduced and reverse remodeling may occur.

Beyond the effects on myocyte hypertrophy, we also observed increased collagen deposition in animals that had received T-1095. As described above, T-1095

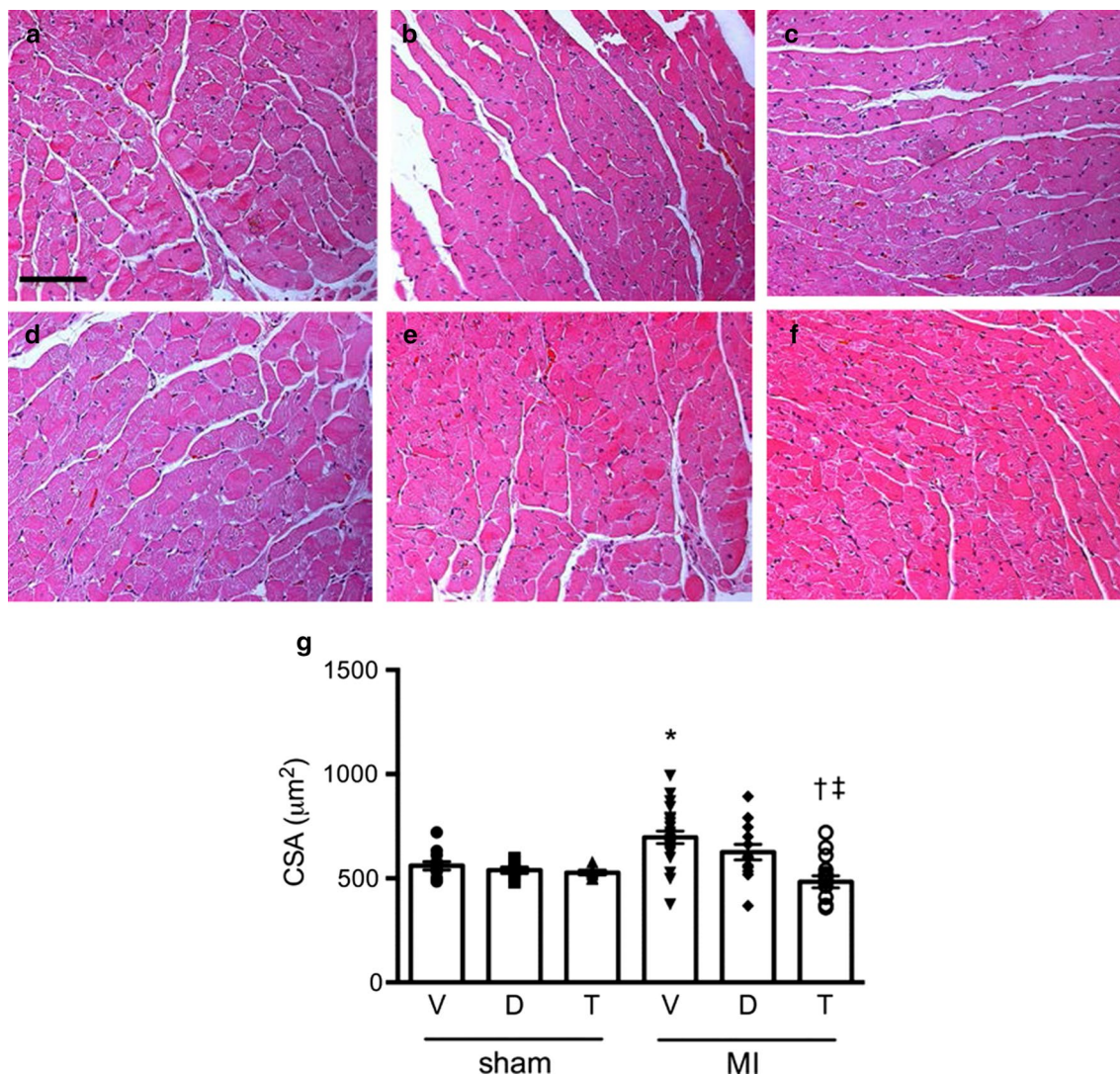


**Fig. 4** Myocyte size. Hematoxylin and eosin-stained cardiac tissue from rats receiving vehicle (a, d), dapagliflozin (b, e) or T-1095 (c, f) in sham (a–c) and post-MI (d–f) settings along with quantitative analysis of myocyte size (g). Animal numbers are provided in Table 1. Scale bar: 100 microns. \* p < 0.05 vs. sham + vehicle, † p < 0.05 vs. MI + vehicle, ‡ p < 0.05 vs. MI + dapagliflozin

mediated inhibition of SGLT1 leads to a diminution in glucose entry that reduces ATP generation, consistent with the reduction in systolic function (EF, dp/dt<sub>max</sub>) and the impairment in the active phase of diastolic relaxation (Tau) reported in the present study. In addition to impaired function, however, the resultant energy depletion would also provide a profibrotic stimulus [45] that would lead to the increase in interstitial collagen.

Phlorizin, the prototypical SGLT1/2 inhibitor is poorly absorbed from the gut so that in addition to a low plasma concentration following oral dosing, its high luminal concentration induces diarrhoea by inhibiting enterocyte SGLT1. To overcome these limitations, we took advantage of T-1095, a phlorizin derivative prodrug that is

readily absorbed from small intestine prior to being converted to its active form, T-1095A, in the systemic circulation [13]. Similar to phlorizin that is a near-equipotent inhibitor of SGLT1 and 2, T-1095A has only a fourfold selectivity for SGLT2 over SGLT1 [14]. In contrast, the three widely-marketed SGLT2 inhibitors, canagliflozin, dapagliflozin and empagliflozin that have SGLT2:SGLT1 selectivity ratios in the order of > 250, > 1200 and > 2500, respectively [46] and while canagliflozin may inhibit gut SGLT1 in clinically used doses [47], its plasma concentration would not be expected to reach levels high enough to inhibit cardiac SGLT1. Beyond canagliflozin, however, drugs with even less selectivity are in development, seeking to capitalise on the theoretical additional glucose



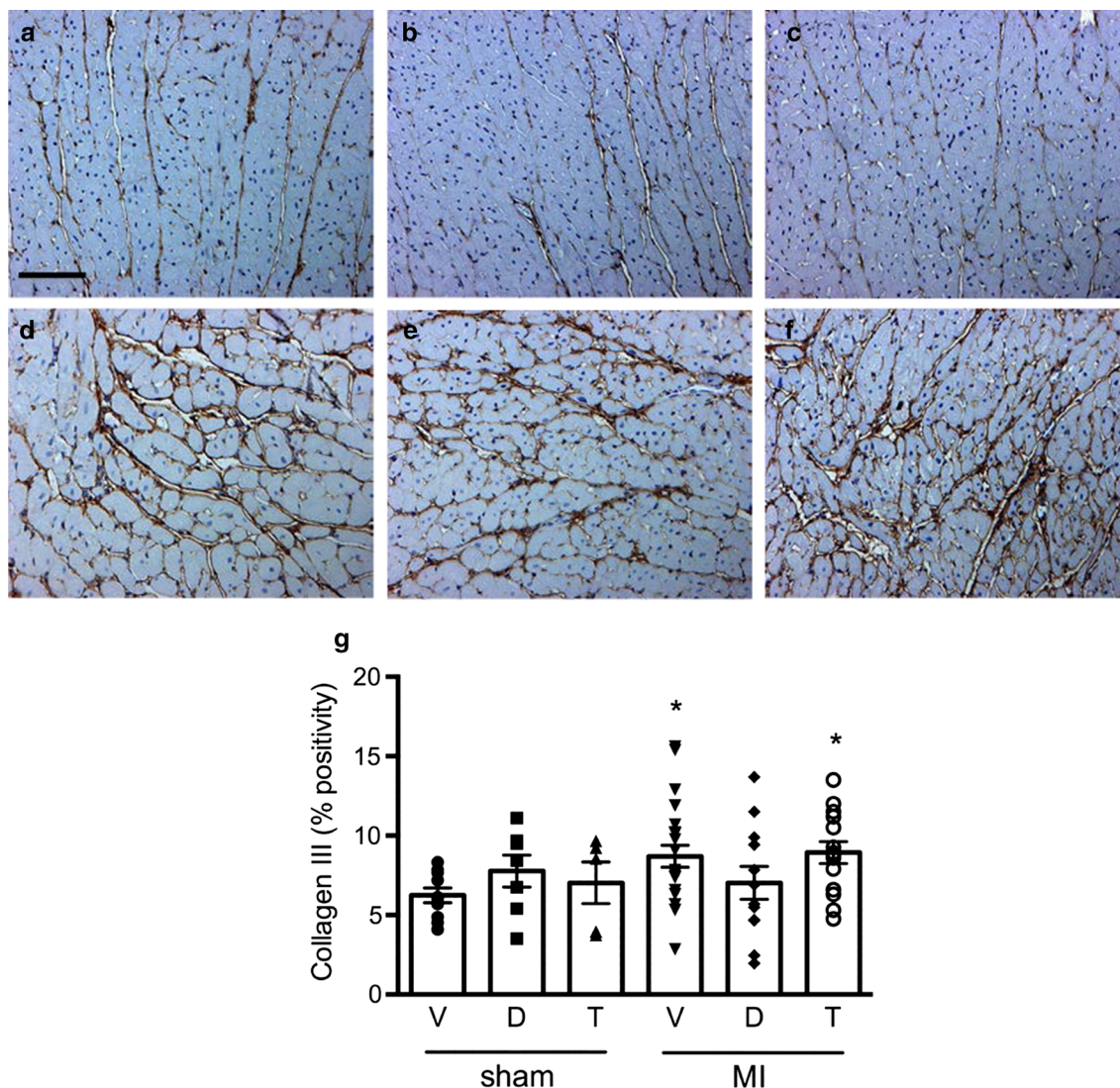


**Fig. 5** Collagen deposition. Immunolabelling of collagen III in hearts from rats receiving vehicle (a, d), dapagliflozin (b, e) or T-1095 (c, f) in sham (a–c) and post-MI (d–f) settings along with quantitative analysis of its abundance (g). Scale bar: 100 microns. \*  $p < 0.05$  vs. sham + vehicle

lowering that may be achieved by inhibiting SGLT1 in the distal segments of the proximal tubule as well as SGLT2 in the more proximal segments [48]. Notably, two drugs designed to inhibit SGLT1 have already entered clinical trials. Sotagloflozin (LX4211) with an  $IC_{50}$  ratio of 20:1 in favour of SGLT2 has completed phase 3 while others such as GSK-1614235 (Glaxo Smith-Kline, PA), designed to preferentially inhibit SGLT1 with an  $IC_{50}$  that is 300-fold less for SGLT1 versus SGLT2, has recently undergone phase 1 clinical testing [49].

The present study has several limitations. First and foremost, while a commonly used model, the abrupt induction of ischemic necrosis in a rodent heart has only superficial resemblance to the myocardial infarction in humans that occurs in the setting of

longstanding atherosclerotic disease, collateral development and in whom a vast array of cardioprotective measures are now employed. Notably, clinical studies of SGLT2 inhibitors have not shown evidence of benefit in being able to reduce the risk of myocardial infarction. As such, the absence of significant improvement in cardiac parameters with dapagliflozin should not be interpreted as an indication that this compound does not prevent hospitalization for heart failure in the clinical setting especially considering the positive findings of its phase 2/3 program [50], post-marketing studies [51] and the effects of other members of the SGLT2 inhibitory class [52] along with supporting basic and translational research studies [53–55]. Secondly, the compound used to inhibit SGLT1/2, T-1095, is not one

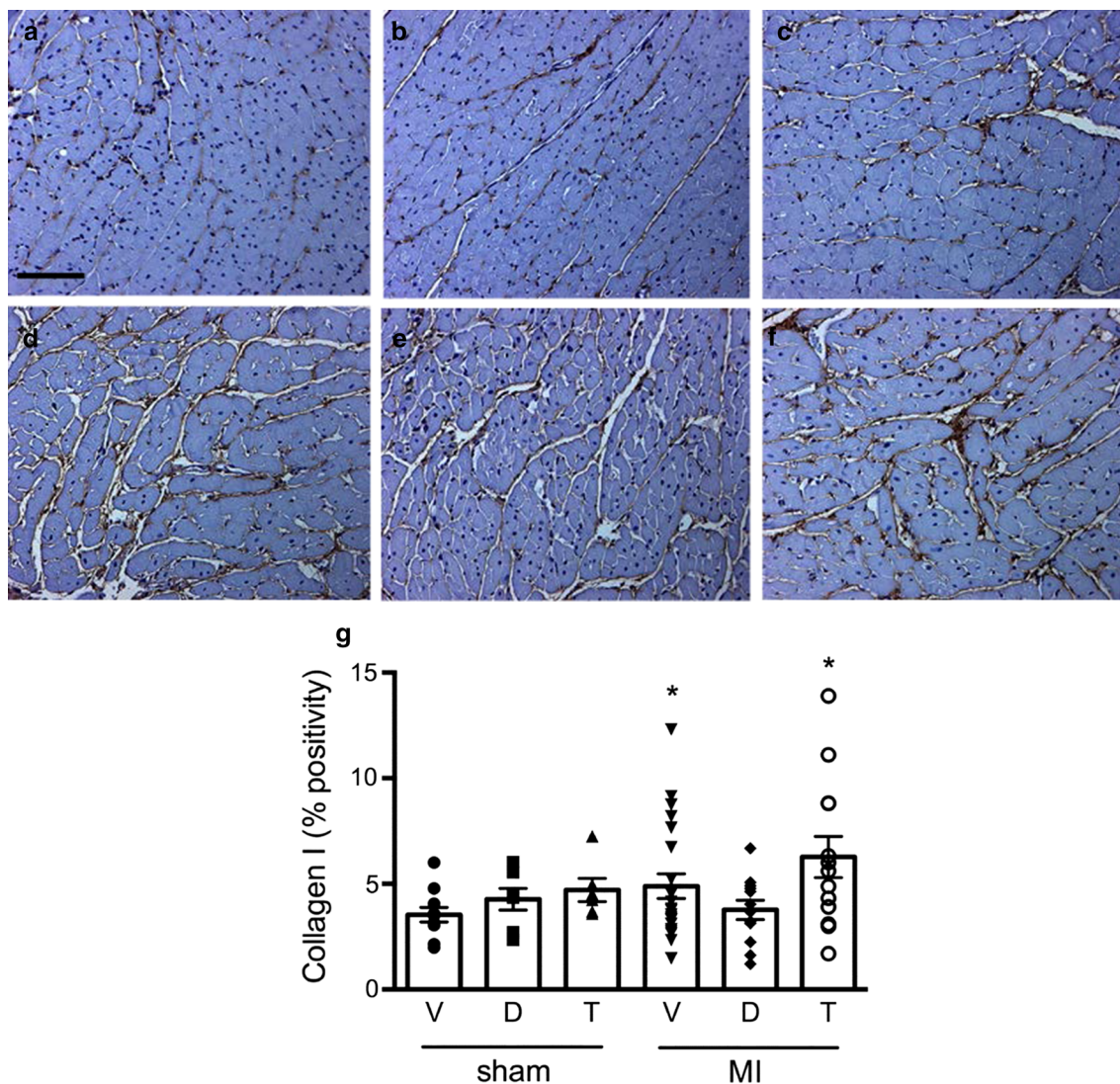


**Fig. 6** Collagen deposition. Immunolabelling of collagen I in hearts from rats receiving vehicle (a, d), dapagliflozin (b, d) or T-1095 (c, e) in sham (a–c) and post-MI (d–f) settings along with quantitative analysis of its abundance (g). Scale bar: 100 microns. \* p < 0.05 vs. sham + vehicle

that is in current use and while the drug was used as a pharmacological probe, extrapolations to other chemical entities may not be warranted. In particular, the combined SGLT1/2 inhibitor, sotagliflozin, as noted previously, has a 20:1 selectivity in favour of SGLT2, contrasting the 4:1 ratio for T-1095.

Although T-1095A's ability to inhibit SGLT1-mediated glucose uptake has been well-documented [13, 14, 16], we did not directly assess glucose transport into the myocardium in the current study. Several other groups have explored the effects of SGLT1 inhibition in heart in cells, atrial strips and using the ex vivo Langendorff technique with T-1095 and phlorizin [10, 11, 38, 56]. These studies demonstrated the importance of SGLT1-mediated

glucose transport in the stress setting whereby its inhibition exacerbates ischemia–reperfusion injury [38, 56]. The novelty and potential clinical relevance of the current study, however, centers on it being the first to examine the effects of SGLT1 inhibition following cardiac injury in the in vivo setting. Notably, given SGLT-mediated effects on preload and afterload [57], we used conductance catheterization that unlike echocardiography provides load-independent measurements of cardiac function in intact animals [25]. While the plasma concentration of T-1095A was not measured in the current study, its effects on SGLT-1 mediated glucose transport can be inferred from the IC<sub>50</sub> for rat SGLT1 of < 1 μM [14] and the plasma concentration of ~ 10 μM that, according to



published pharmacokinetic for the compound, would have been attained with the doses used [58]. Finally, although a direct effect of T-1095 on cardiac SGLT1 provides a cogent explanation for the observed effects, it is conceivable that altered glucose transport in other cells that express SGLT1 might have contributed, including the cardiac capillary endothelium [4].

## Conclusions

The exacerbation of post myocardial infarction cardiac dysfunction with T-1095 in the experimental setting suggests the need for caution with the use of dual SGLT1/2 inhibitors in humans, reinforcing the prudent approach taken by regulatory authorities in specifically studying patients with cardiovascular disease before bringing a new glucose-lowering drug to market.

## Abbreviations

ANP: atrial natriuretic peptide; BG: blood glucose; BP: blood pressure; BW: body weight;  $dP/dt_{max}$ : rate of left ventricle (LV) pressure during isovolumic contraction;  $dP/dt_{min}$ : ( $-dP/dt$ ) pressure fall during isovolumic relaxation; EDPVR: end-diastolic pressure volume relationship; EF: ejection fraction; FS: fractional shortening; LAD: left anterior descending coronary artery; MI: myocardial infarction; SGLT: sodium–glucose linked cotransporter; TL: tibial length.

## Authors' contributions

KAC conceived of the study, analyzed the echocardiographic and conductance catheter data and reviewed and approved the final version of the manuscript. KT performed molecular and histological analyses and reviewed and approved the final version of the manuscript. YZ performed histological and statistical analyses and reviewed and approved the final version of the manuscript. J-FD, performed animal surgery, echocardiography and conductance catheterization and reviewed and approved the final version of the manuscript. REG conceived of the study and wrote the manuscript and reviewed. All authors read and approved the final manuscript.

## Acknowledgements

The authors are grateful for the assistance of Jennifer Switzer for her excellent animal care and Lei Cai for her excellent assistance with histology.

## Competing interests

KAC has received research grants to his institution from Astra Zeneca and Boehringer Ingelheim, received support for travel to scientific meeting from Boehringer Ingelheim and honoraria for speaking engagements and ad hoc participation in advisory boards from Astra Zeneca, Boehringer Ingelheim and Janssen. REG has received research grants to his institution from Astra Zeneca and Boehringer Ingelheim, received support for travel to scientific meeting from Astra Zeneca and honoraria for speaking engagements and ad hoc participation in advisory boards from Astra Zeneca, Boehringer Ingelheim and Janssen. The authors declare that they have no competing interests.

## Availability of data and materials

The datasets used and/or analysed during the current study are available from the corresponding author on reasonable request.

## Consent for publication

This study consists of animal and cell culture data and is devoid of any human data.

## Ethics approval and consent to participate

All animal studies were approved by the St. Michael's Hospital Animal Care Committee in accordance with the Guide for the Care and Use of Laboratory Animals (NIH Publication No. 85-23, revised 1996).

## Funding

Studies were supported by research grants from the St. Michael's Hospital Foundation and Astra Zeneca. Dr. Gilbert is the Canada Research Chair in Diabetes Complication and this research was made possible, in part, by the Canada Research Chair's Program. Dr. KA Connelly is supported by a New Investigator reward from the Canadian Institute of Heart and circulatory research and an Early researcher award from the Ministry of Ontario.

## Publisher's Note

Springer Nature remains neutral with regard to jurisdictional claims in published maps and institutional affiliations.

Received: 12 March 2018 Accepted: 2 July 2018

Published online: 07 July 2018

## References

- Zinman B, Wanner C, Lachin JM, Fitchett D, Bluhmki E, Hantel S, Matthews M, Devins T, Johansen OE, Woerle HJ, et al. Empagliflozin, cardiovascular outcomes, and mortality in type 2 diabetes. *N Engl J Med*. 2015;373:2117–28.
- Neal B, Perkovic V, Mahaffey KW, de Zeeuw D, Fulcher G, Erondu N, Shaw W, Law G, Desai M, Matthews DR, et al. Canagliflozin and cardiovascular and renal events in type 2 diabetes. *N Engl J Med*. 2017;377(7):644–57.
- Song P, Onishi A, Koepsell H, Vallon V. Sodium glucose cotransporter SGLT1 as a therapeutic target in diabetes mellitus. *Expert Opin Ther Targets*. 2016;20(9):1109–25.
- Vrhovac I, Balen Erer D, Klessen D, Burger C, Brejcek D, Kraus O, Radovic N, Jadrijevic S, Aleksic I, Walles T, et al. Localizations of Na(+)-D-glucose cotransporters SGLT1 and SGLT2 in human kidney and of SGLT1 in human small intestine, liver, lung, and heart. *Pflugers Arch*. 2015;467(9):1881–98.
- Chen J, Williams S, Ho S, Loraine H, Hagan D, Whaley JM, Feder JN. Quantitative PCR tissue expression profiling of the human SGLT2 gene and related family members. *Diab Ther*. 2010;1(2):57–92.
- Bonner C, Kerr-Conte J, Gmyr V, Queniat G, Moerman E, Thevenet J, Beaucamps C, Delalleau N, Popescu I, Malaise WJ, et al. Inhibition of the glucose transporter SGLT2 with dapagliflozin in pancreatic alpha cells triggers glucagon secretion. *Nat Med*. 2015;21(5):512–7.
- Van Steenberghe A, Balteau M, Ginion A, Ferte L, Battault S, Ravenstein CM, Balligand JL, Daskalopoulos EP, Gilon P, Despa F, et al. Sodium-myoinositol cotransporter-1, SMIT1, mediates the production of reactive oxygen species induced by hyperglycemia in the heart. *Sci Rep*. 2017;7:41166.
- Lopaschuk GD, Ussher JR, Folmes CD, Jaswal JS, Stanley WC. Myocardial fatty acid metabolism in health and disease. *Physiol Rev*. 2010;90(1):207–58.
- Schwenk RW, Luiken JJ, Bonen A, Glatz JF. Regulation of sarcolemmal glucose and fatty acid transporters in cardiac disease. *Cardiovasc Res*. 2008;79(2):249–58.
- Kashiwagi Y, Nagoshi T, Yoshino T, Tanaka TD, Ito K, Harada T, Takahashi H, Ikegami M, Anzawa R, Yoshimura M. Expression of SGLT1 in human hearts and impairment of cardiac glucose uptake by phlorizin during ischemia-reperfusion injury in mice. *PLoS ONE*. 2015;10(6):e0130605.
- Banerjee SK, McGaffin KR, Pastor-Soler NM, Ahmad F. SGLT1 is a novel cardiac glucose transporter that is perturbed in disease states. *Cardiovasc Res*. 2009;84(1):111–8.
- Zhou L, Cryan EV, D'Andrea MR, Belkowsky S, Conway BR, Demarest KT. Human cardiomyocytes express high level of Na+/glucose cotransporter 1 (SGLT1). *J Cell Biochem*. 2003;90(2):339–46.
- Tsujiyama K, Hongu M, Saito K, Kawanishi H, Kuriyama K, Matsumoto M, Oku A, Ueta K, Tsuda M, Saito A. Na(+)-glucose cotransporter (SGLT) inhibitors as antidiabetic agents. 4. Synthesis and pharmacological properties of 4'-dehydroxyphlorizin derivatives substituted on the B ring. *J Med Chem*. 1999;42(26):5311–24.
- Oku A, Ueta K, Arakawa K, Ishihara T, Nawano M, Kuronuma Y, Matsumoto M, Saito A, Tsujihara K, Anai M, et al. T-1095, an inhibitor of renal Na+–glucose cotransporters, may provide a novel approach to treating diabetes. *Diabetes*. 1999;48(9):1794–800.

15. Pfeffer MA, Pfeffer JM, Fishbein MC, Fletcher PJ, Spadaro J, Kloner RA, Braunwald E. Myocardial infarct size and ventricular function in rats. *Circ Res*. 1979;44(4):503–12.
16. Asano T, Ogihara T, Katagiri H, Sakoda H, Ono H, Fujishiro M, Anai M, Kurihara H, Uchijima Y. Glucose transporter and Na<sup>+</sup>/glucose cotransporter as molecular targets of anti-diabetic drugs. *Curr Med Chem*. 2004;11(20):2717–24.
17. Zhang Y, Thai K, Kepecs DM, Gilbert RE. Sodium–glucose linked cotransporter-2 inhibition does not attenuate disease progression in the rat remnant kidney model of chronic kidney disease. *PLoS ONE*. 2016;11(1):e0144640.
18. Han S, Hagan DL, Taylor JR, Xin L, Meng W, Biller SA, Wetterau JR, Washburn WN, Whaley JM. Dapagliflozin, a selective SGLT2 inhibitor, improves glucose homeostasis in normal and diabetic rats. *Diabetes*. 2008;57(6):1723–9.
19. Adachi T, Yasuda K, Okamoto Y, Shihara N, Oku A, Ueta K, Kitamura K, Saito A, Iwakura I, Yamada Y, et al. T-1095, a renal Na<sup>+</sup>–glucose transporter inhibitor, improves hyperglycemia in streptozotocin-induced diabetic rats. *Metabolism*. 2000;49(8):990–5.
20. Boyle AJ, Kelly DJ, Zhang Y, Cox AJ, Gow RM, Way K, Itescu S, Krum H, Gilbert RE. Inhibition of protein kinase C reduces left ventricular fibrosis and dysfunction following myocardial infarction. *J Mol Cell Cardiol*. 2005;39(2):213–21.
21. Morgan EE, Faulx MD, McElfresh TA, Kung TA, Zawaneh MS, Stanley WC, Chandler MP, Hoit BD. Validation of echocardiographic methods for assessing left ventricular dysfunction in rats with myocardial infarction. *Am J Physiol Heart Circ Physiol*. 2004;287(5):H2049–53.
22. Ramunddal T, Lorentzon M, Omerovic E. Decreased mortality in a rat model of acute postinfarction heart failure. *Biochem Biophys Res Commun*. 2006;341(2):459–63.
23. Yin FC, Spurgeon HA, Rakusan K, Weisfeldt ML, Lakatta EG. Use of tibial length to quantify cardiac hypertrophy: application in the aging rat. *Am J Physiol*. 1982;243(6):H941–7.
24. Tan SM, Zhang Y, Connelly KA, Gilbert RE, Kelly DJ. Targeted inhibition of activin receptor-like kinase 5 signaling attenuates cardiac dysfunction following myocardial infarction. *Am J Physiol Heart Circ Physiol*. 2010;298(5):H1415–25.
25. Connelly KA, Prior DL, Kelly DJ, Feneley MP, Krum H, Gilbert RE. Load-sensitive measures may overestimate global systolic function in the presence of left ventricular hypertrophy: a comparison with load-insensitive measures. *Am J Physiol Heart Circ Physiol*. 2006;290(4):H1699–705.
26. Devereux RB, Reichek N. Echocardiographic determination of left ventricular mass in man. Anatomic validation of the method. *Circulation*. 1977;55(4):613–8.
27. Lang RM, Badano LP, Mor-Avi V, Afilalo J, Armstrong A, Ernande L, Flachskampf FA, Foster E, Goldstein SA, Kuznetsova T, et al. Recommendations for cardiac chamber quantification by echocardiography in adults: an update from the American Society of Echocardiography and the European Association of Cardiovascular Imaging. *J Am Soc Echocardiogr*. 2015;28(1):1–39.
28. Derumeaux G, Mulder P, Richard V, Chagraoui A, Nafeh C, Bauer F, Henry JP, Thuillez C. Tissue Doppler imaging differentiates physiological from pathological pressure-overload left ventricular hypertrophy in rats. *Circulation*. 2002;105(13):1602–8.
29. Zhang Y, Connelly KA, Thai K, Wu X, Kapus A, Kepecs D, Gilbert RE. Sirtuin 1 activation reduces transforming growth factor-beta 1-induced fibrogenesis and affords organ protection in a model of progressive, experimental kidney and associated cardiac disease. *Am J Pathol*. 2017;187(1):80–90.
30. Connelly KA, Zhang Y, Advani A, Advani SL, Thai K, Yuen DA, Gilbert RE. DPP-4 inhibition attenuates cardiac dysfunction and adverse remodeling following myocardial infarction in rats with experimental diabetes. *Cardiovasc Ther*. 2013;31(5):259–67.
31. Connelly KA, Kelly DJ, Zhang Y, Prior DL, Advani A, Cox AJ, Thai K, Krum H, Gilbert RE. Inhibition of protein kinase C-beta by ruboxistaurin preserves cardiac function and reduces extracellular matrix production in diabetic cardiomyopathy. *Circ Heart Fail*. 2009;2(2):129–37.
32. Connelly KA, Advani A, Kim S, Advani SL, Zhang M, White KE, Kim YM, Parker C, Thai K, Krum H, et al. The cardiac (pro)renin receptor is primarily expressed in myocyte transverse tubules and is increased in experimental diabetic cardiomyopathy. *J Hypertens*. 2011;29(6):1175–84.
33. Kosanam H, Thai K, Zhang Y, Advani A, Connelly KA, Diamandis EP, Gilbert RE. Diabetes induces lysine acetylation of intermediary metabolism enzymes in the kidney. *Diabetes*. 2014;63(7):2432–9.
34. Connelly KA, Kelly DJ, Zhang Y, Prior DL, Martin J, Cox AJ, Thai K, Feneley MP, Tsoporis J, White KE, et al. Functional, structural and molecular aspects of diastolic heart failure in the diabetic (mRen-2)27 rat. *Cardiovasc Res*. 2007;76(2):280–91.
35. Opie LH, Commerford PJ, Gersh BJ, Pfeffer MA. Controversies in ventricular remodelling. *Lancet*. 2006;367(9507):356–67.
36. Mirtschink P, Krek W. Hypoxia-driven glycolytic and fructolytic metabolic programs: pivotal to hypertrophic heart disease. *Biochim Biophys Acta*. 2016;1863(7 Pt B):1822–8.
37. Banerjee SK, Wang DW, Alzamora R, Huang XN, Pastor-Soler NM, Hallows KR, McGaffin KR, Ahmad F. SGLT1, a novel cardiac glucose transporter, mediates increased glucose uptake in PRKAG2 cardiomyopathy. *J Mol Cell Cardiol*. 2010;49(4):683–92.
38. Kanwal A, Nizami HL, Mallapudi S, Putcha UK, Mohan GK, Banerjee SK. Inhibition of SGLT1 abrogates preconditioning-induced cardioprotection against ischemia-reperfusion injury. *Biochem Biophys Res Commun*. 2016;472(2):392–8.
39. Crozatier B, Ventura-Clapier R. Inhibition of hypertrophy, per se, may not be a good therapeutic strategy in ventricular pressure overload: other approaches could be more beneficial. *Circulation*. 2015;131(16):1448–57.
40. Meguro T, Hong C, Asai K, Takagi G, McKinsey TA, Olson EN, Vatner SF. Cyclosporine attenuates pressure-overload hypertrophy in mice while enhancing susceptibility to decompensation and heart failure. *Circ Res*. 1999;84(6):735–40.
41. Rogers JH, Tamirisa P, Kovacs A, Weinheimer C, Courtois M, Blumer KJ, Kelly DP, Muslin AJ. RGS4 causes increased mortality and reduced cardiac hypertrophy in response to pressure overload. *J Clin Invest*. 1999;104(5):567–76.
42. Braccaccio M, Fratta L, Notte A, Hirsch E, Poulet R, Guazzone S, De Acetis M, Vecchione C, Marino G, Altruda F, et al. Melusin, a muscle-specific integrin beta1-interacting protein, is required to prevent cardiac failure in response to chronic pressure overload. *Nat Med*. 2003;9(1):68–75.
43. Gelpi RJ, Gao S, Zhai P, Yan L, Hong C, Danridge LM, Ge H, Maejima Y, Donato M, Yokota M, et al. Genetic inhibition of calcineurin induces diastolic dysfunction in mice with chronic pressure overload. *Am J Physiol Heart Circ Physiol*. 2009;297(5):H1814–9.
44. Rothenmel BA, Berenji K, Tannous P, Kutschke W, Dey A, Nolan B, Yoo KD, Demetroulis E, Gimbel M, Cabuay B, et al. Differential activation of stress-response signaling in load-induced cardiac hypertrophy and failure. *Physiol Genomics*. 2005;23(1):18–27.
45. Gonzalez A, Schelbert EB, Diez J, Butler J. Myocardial interstitial fibrosis in heart failure: biological and translational perspectives. *J Am Coll Cardiol*. 2018;71(15):1696–706.
46. Riser Taylor S, Harris KB. The clinical efficacy and safety of sodium glucose cotransporter-2 inhibitors in adults with type 2 diabetes mellitus. *Pharmotherapy*. 2013;33(9):984–99.
47. Polidori D, Sha S, Mudaliar S, Ciaraldi TP, Ghosh A, Vaccaro N, Farrell K, Rothenberg P, Henry RR. Canagliflozin lowers postprandial glucose and insulin by delaying intestinal glucose absorption in addition to increasing urinary glucose excretion: results of a randomized, placebo-controlled study. *Diabetes Care*. 2013;36(8):2154–61.
48. Chao EC, Henry RR. SGLT2 inhibition—a novel strategy for diabetes treatment. *Nat Rev Drug Discov*. 2010;9(7):551–9.
49. Dobbins RL, Greenway FL, Chen L, Liu Y, Breed SL, Andrews SM, Wald JA, Walker A, Smith CD. Selective sodium-dependent glucose transporter 1 inhibitors block glucose absorption and impair glucose-dependent insulinotropic peptide release. *Am J Physiol Gastrointest Liver Physiol*. 2015;308(11):G946–54.
50. Gilbert RE, Krum H. Heart failure in diabetes: effects of anti-hyperglycaemic drug therapy. *Lancet*. 2015;385(9982):2107–17.
51. Kosiborod M, Cavender MA, Norhammar A, Wilding J, Khunti K. Lower rates of hospitalization for heart failure and all-cause death in new users of sglT2 inhibitors: the CVD-REAL study. In: 66th scientific session of the American College of Cardiology. Washington, DC; 2017 (**Abstract 415–414**)
52. Zinman B, Lachin JM, Inzucchi SE. Empagliflozin, cardiovascular outcomes, and mortality in type 2 diabetes. *N Engl J Med*. 2016;374(11):1094.



53. Kusaka H, Koibuchi N, Hasegawa Y, Ogawa H, Kim-Mitsuyama S. Empagliflozin lessened cardiac injury and reduced visceral adipocyte hypertrophy in prediabetic rats with metabolic syndrome. *Cardiovasc Diabetol*. 2016;15(1):157.
54. Lee TM, Chang NC, Lin SZ. Dapagliflozin, a selective SGLT2 Inhibitor, attenuated cardiac fibrosis by regulating the macrophage polarization via STAT3 signaling in infarcted rat hearts. *Free Radic Biol Med*. 2017;104:298–310.
55. Habibi J, Aroor AR, Sowers JR, Jia G, Hayden MR, Garro M, Barron B, Mayoux E, Rector RS, Whaley-Connell A, et al. Sodium glucose transporter 2 (SGLT2) inhibition with empagliflozin improves cardiac diastolic function in a female rodent model of diabetes. *Cardiovasc Diabetol*. 2017;16(1):9.
56. von Lewinski D, Rainer PP, Gasser R, Huber MS, Khafaga M, Wilhelm B, Haas T, Machler H, Rossl U, Pieske B. Glucose-transporter-mediated positive inotropic effects in human myocardium of diabetic and nondiabetic patients. *Metabolism*. 2010;59(7):1020–8.
57. Lytvyn Y, Bjornstad P, Udell JA, Lovshin JA, Cherney DZI. Sodium glucose cotransporter-2 inhibition in heart failure: potential mechanisms, clinical applications, and summary of clinical trials. *Circulation*. 2017;136(17):1643–58.
58. Yamaguchi K, Kato M, Ozawa K, Kawai T, Yata T, Aso Y, Ishigai M, Ikeda S. Pharmacokinetic and pharmacodynamic modeling for the effect of sodium–glucose cotransporter inhibitors on blood glucose level and renal glucose excretion in db/db mice. *J Pharm Sci*. 2012;101(11):4347–56.

Ready to submit your research? Choose BMC and benefit from:

- fast, convenient online submission
- thorough peer review by experienced researchers in your field
- rapid publication on acceptance
- support for research data, including large and complex data types
- gold Open Access which fosters wider collaboration and increased citations
- maximum visibility for your research: over 100M website views per year

At BMC, research is always in progress.

Learn more [biomedcentral.com/submissions](https://biomedcentral.com/submissions)

